



HAL
open science

Influence of neodymium concentration on excitation and emission properties of Nd doped gallium oxide nanocrystalline films

A Podhorodecki, M Banski, J Misiewicz, Céline Lecerf, P Marie, J. Cardin, X Portier

► To cite this version:

A Podhorodecki, M Banski, J Misiewicz, Céline Lecerf, P Marie, et al.. Influence of neodymium concentration on excitation and emission properties of Nd doped gallium oxide nanocrystalline films. Journal of Applied Physics, 2010, 108 (6), pp.063535. 10.1063/1.3484039 . hal-01139768

HAL Id: hal-01139768

<https://hal.science/hal-01139768>

Submitted on 7 Apr 2015

HAL is a multi-disciplinary open access archive for the deposit and dissemination of scientific research documents, whether they are published or not. The documents may come from teaching and research institutions in France or abroad, or from public or private research centers.

L'archive ouverte pluridisciplinaire **HAL**, est destinée au dépôt et à la diffusion de documents scientifiques de niveau recherche, publiés ou non, émanant des établissements d'enseignement et de recherche français ou étrangers, des laboratoires publics ou privés.



Distributed under a Creative Commons Attribution - NonCommercial - NoDerivatives 4.0 International License

Influence of neodymium concentration on excitation and emission properties of Nd doped gallium oxide nanocrystalline films

A. Podhorodecki, M. Banski, J. Misiewicz, C. Lecerf, P. Marie, J. Cardin, and X. Portier

Citation: [Journal of Applied Physics](#) **108**, 063535 (2010); doi: 10.1063/1.3484039

View online: <http://dx.doi.org/10.1063/1.3484039>

View Table of Contents: <http://scitation.aip.org/content/aip/journal/jap/108/6?ver=pdfcov>

Published by the [AIP Publishing](#)

Articles you may be interested in

[Investigation on the compensation effect of residual carbon impurities in low temperature grown Mg doped GaN films](#)

J. Appl. Phys. **115**, 163704 (2014); 10.1063/1.4873957

[Elevated temperature dependent transport properties of phosphorus and arsenic doped zinc oxide thin films](#)

J. Appl. Phys. **114**, 223709 (2013); 10.1063/1.4845855

[Improvement of \(004\) texturing by slow growth of Nd doped TiO₂ films](#)

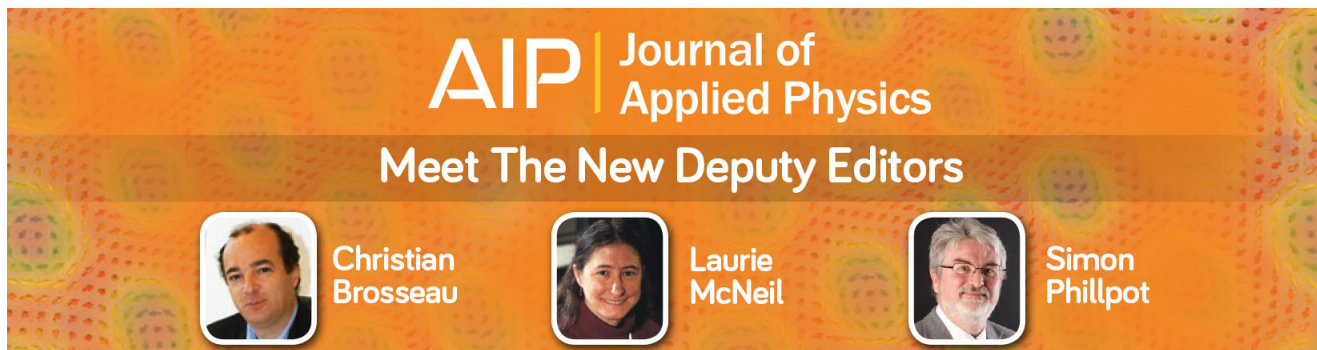
J. Appl. Phys. **112**, 113505 (2012); 10.1063/1.4767361

[Visible light emission and energy transfer processes in Sm-doped nitride films](#)

J. Appl. Phys. **111**, 123105 (2012); 10.1063/1.4729911

[Arsenic doped p-type zinc oxide films grown by radio frequency magnetron sputtering](#)

J. Appl. Phys. **106**, 073709 (2009); 10.1063/1.3236578



AIP | Journal of Applied Physics

Meet The New Deputy Editors

	Christian Brosseau		Laurie McNeil		Simon Phillpot
---	---------------------------	---	----------------------	---	-----------------------

Influence of neodymium concentration on excitation and emission properties of Nd doped gallium oxide nanocrystalline films

A. Podhorodecki,^{1,a)} M. Banski,¹ J. Misiewicz,¹ C. Lecerf,² P. Marie,² J. Cardin,² and X. Portier²

¹*Institute of Physics, Wrocław University of Technology, Wybrzeże Wyspińskiego 27, 50-370 Wrocław, Poland*

²*CIMAP, CEA/UMR CNRS 6252/ENSICAEN, Université de Caen Basse Normandie, 6 Boulevard Maréchal Juin, 14050 Caen, France*

(Received 2 July 2010; accepted 29 July 2010; published online 24 September 2010)

Gallium oxide and more particularly β -Ga₂O₃ matrix is an excellent material for new generation of devices electrically or optically driven as it is known as the widest band gap transparent conductive oxide. In this paper, the optical properties of neodymium doped gallium oxide films grown by magnetron sputtering have been analyzed. The influence of the Nd ions concentration on the excitation/emission mechanisms of Nd ions and the role of gallium oxide matrix have been investigated. The grain size reduction into gallium oxide films have been observed when concentration of Nd increases. It has been found for all samples that the charge transfer is the main excitation mechanism for Nd ions where defect states play an important role as intermediate states. As a consequence Nd emission efficiency increases with temperature giving rise to most intensive emission at 1087 nm at room temperature. © 2010 American Institute of Physics. [doi:10.1063/1.3484039]

I. INTRODUCTION

Light emitting diodes or laser sources working in the near infrared region are under extensive investigation due to a wide range of their potential applications. Among many different solutions like quantum wells,¹ quantum dashes,² or quantum dots,³ and doping or codoping of semiconductors by rare earth (RE), i.e., Nd, Er ions^{4,5} gives many new opportunities for infrared light sources. Their exceptional properties arise from the fact that their optical transitions take place among internal $4f$ orbitals, which are shielded from the environment by $5d$ -orbital electrons. It results in an emission with a narrow band and extremely stable wavelength, regardless in some extent of the external conditions in matrix transparent in the wide spectral range. In addition, this concept gives many other new possibilities since this kind of matrices can be easily codoped by other ions covering a spectral range from 400–2000 nm.⁶

However, the main limitation of RE ions is their small absorption cross section due to electric dipole transitions which are forbidden according to Laporte's rule. In addition, their low solubility in the matrix is reflected as ions clustering which quenches their emission above critical, often very low (less than 0.1%), RE content. Thus, in order to increase their emission efficiency, crucial for practical applications, their excitation should be sensitized by an additional donor center, i.e., matrix,⁷ defects states,⁸ nanocrystals,⁴ or other molecules, i.e., molecular oxygen.⁹ At these limited conditions for using RE ions as emitters in real devices, a better understanding of the excitation and quenching mechanisms should be investigated in details to optimize their optical properties.

The other important issue, to overcome for this kind of “discrete” light emitters is the poor electrical properties of matrices used as a RE ions host. Thus, even if optical pumping of RE ions via the energy transfer gives promising results, electrical pumping became very difficult to realize in practice.

In the following, gallium oxide films were used as a host matrix of Nd³⁺ ions. This material is well known as a transparent conductive oxide with the widest band gap (4.9 eV), which can exhibit n-type semiconductor properties in case of some oxygen deficiency.¹⁰ Thus, this material is a promising matrix for next generation optoelectronic devices working in a longer wavelength. Due to its low maximum phonon energy (~ 793 cm⁻¹) (Ref. 11) as compared to silicate glasses (~ 1100 cm⁻¹), and its high refractive index ($n=1.96$ at 1.06 μm) (Ref. 12) it is expected to provide significantly high radiative decay rates and low nonradiative relaxation rates of RE excited-state levels. RE-doped gallium oxide is also a promising material for electroluminescent based devices.^{13–16} Additionally, this matrix can exhibit good electrical properties when doped within.¹⁷

In the present work, gallium oxide films doped with various Nd³⁺ concentrations have been investigated to determine their excitation mechanism and its evolution versus Nd content in the matrix. The absorption, photoluminescence (PL) and photoluminescence excitation (PLE) measurements in the wide temperature range of 10–300 K have been performed for all the samples.

II. EXPERIMENTAL DETAILS

The neodymium doped gallium oxide films have been elaborated by magnetron sputtering of a Ga₂O₃ target (99.99% purity) partially covered by Nd₂O₃ (99.99% purity)

^{a)}Electronic mail: artur.p.podhorodecki@pwr.wroc.pl.

pellets of calibrated shapes. Nd^{3+} concentration varies with the r parameter, corresponding to the Nd_2O_3 pellets-to- Ga_2O_3 target surface ratio. The samples investigated in our study had r in the range 0%–38.8%. The layers were grown on p doped and (100)-oriented Si substrates. During all the growth process, the 100 °C temperature was kept constant. Post annealing treatments were carried out at 1000 °C during 1 h under a continuous flow of nitrogen. A more detailed description of the sample preparation was already presented in a previous article.¹⁸

Rutherford backscattering spectroscopy (RBS) experiments were performed using a $^4\text{He}^+$ ion beam with a 2.5 MeV Van de Graaff accelerator of the “Institut des Nano-sciences de Paris.”

Transmission electron microscope (TEM) observations of the films were carried out using a JEOL 2010F TEM operated at 200 kV. Dark field images and high resolution TEM images were taken along the [110] direction of the Si substrate. This direction allows a cross sectional view of the samples with the beam parallel to the film/substrate interface.

Regarding the optical properties of the films, for PLE spectroscopy, samples were excited by a xenon lamp (450 W) coupled with a monochromator (Jobin Yvon TRIAX 180) and for absorbance measurements, a tungsten–deuterium halogen lamp was used. The visible PL, absorbance, and PLE signals were collected and transmitted by an optical fiber to the spectrometer (HR4000 Ocean Optics) and divided by the light source characteristic. The PL spectra in the infrared spectral range were obtained by cooled linear In-GaAs array detector of 512 pixels coupled to the monochromator (Jobin Yvon TRIAX 550).

III. RESULTS AND DISCUSSION

The relationship between r values and Nd contents in the films has been established thanks to RBS measurements from as-deposited films, in which the Nd distribution is supposed to be homogeneous. Obtained in this way values are equal to 0.08 at. %, 0.94 at. %, 1.56 at. %, and 1.79 at. % of Nd for $r=24.2$, 29.1, 33.9 and 38.8, respectively. Also, secondary ion mass spectroscopy experiments are in progress and complementary results will be published in a forthcoming publication.¹⁹

As it has been already shown in previous works,²⁰ all as-grown films are amorphous. Upon annealing treatment at 1000 °C, the films become mostly crystalline. TEM images of cross-section views of annealed gallium oxide films are shown in Fig. 1. Figures 1(a) and 1(c) correspond to a film grown with $r=9.7\%$, which is equivalent to a Nd^{3+} atomic concentration lower than 0.08%. The images show a rather good crystallinity of the film with a columnar growth more particularly in the upper part of the film [Fig. 1(c)]. In the bottom part of the film [Fig. 1(a)], relatively large grains are visible with no texture or columnar structure. The average grain size is approximately 55 nm, but the size distribution is large (from 10 up to 100 nm). It is worth noting that voids (brightest regions in the image) are also present in the film as well as amorphous regions (gray regions). Figure 1(b) presents a bright field TEM image of a sample prepared with

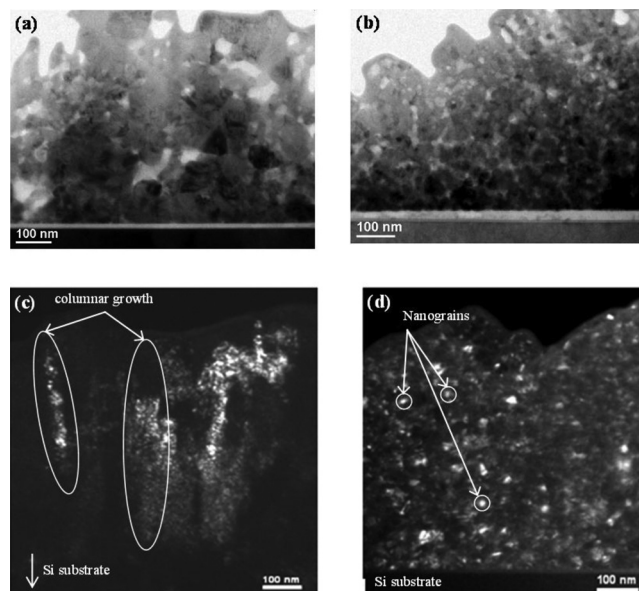


FIG. 1. Bright field TEM images of annealed samples elaborated with (a) $r=9.7\%$ and (b) $r=38.8\%$. Dark field TEM images of the corresponding r values (c) and (d), respectively. In the first case, columnar growth and relatively large grains are observed whereas in the latter case, a random growth prevails with a concomitant nanostructuring of the film.

1.79% of Nd ions. A dark field image of this sample is also reported in Fig. 1(d). In this case, the average grain size is about 10 nm and then much smaller than the previous case. It is also interesting to notice that the grain size is more uniform.

In our previous article,²⁰ x-ray diffraction experiments demonstrated the formation of the stable $\beta\text{-Ga}_2\text{O}_3$ phase for all r values upon annealing. This result was confirmed by high resolution TEM (HREM) observations of well oriented grains whose patterns were consistent with the above mentioned structure. However, RBS experiments have revealed that, for low r values, the expected gallium oxide stoichiometry (Ga_2O_3) is not reached and this was observed for both as-deposited and annealed films. Indeed, the stoichiometry evolves from $\text{Ga}_2\text{O}_{2.7}$ for low r values and tends to the expected Ga_2O_3 alloy for higher r values.

These results mean that, despite the formation of the $\beta\text{-Ga}_2\text{O}_3$ phase in all cases, a more pronounced oxygen deficiency is observed for low r values. Furthermore, a high degree of Nd doping favors the formation of $\beta\text{-Ga}_2\text{O}_3$ nanoparticles.

Regarding Nd localization in the film, local energy dispersive x-ray diffraction (EDX) experiments have been attempted for both samples of Fig. 1. No variation in the Nd concentration has been noticed for the lowest r value (9.7%). A more particular attention has been paid to grain boundaries but the Nd concentration remained lower than the detection limit of the spectrometer. Concerning the highest r value, significant Nd concentrations (up to 7%) have been noticed around the $\beta\text{-Ga}_2\text{O}_3$ nanoparticles confirming a nonuniform distribution of the RE in the film and a pronounced presence of Nd in the surrounding of the $\beta\text{-Ga}_2\text{O}_3$ nanoparticles. By contrast, local composition measurements in the grains lead to a Nd concentration varying from 1.5 up to 2%.

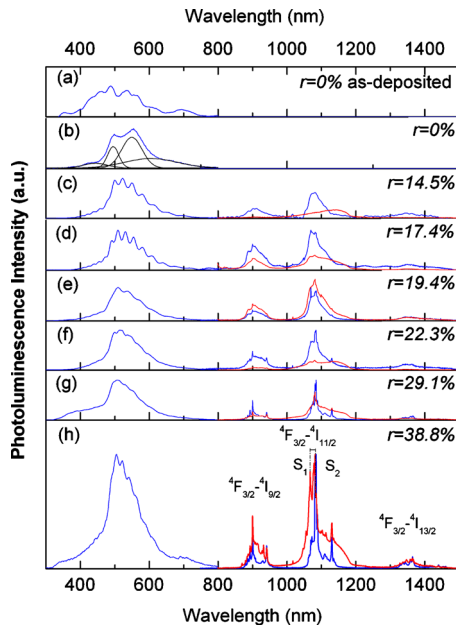


FIG. 2. (Color online) PL spectra obtained for Nd doped gallium oxide films at two different excitation wavelengths: 266 (blue line) and 787 nm (red line). All films have been annealed, excluded the one related to the (a) spectra. (Scales have been adapted for better view).

Figure 2 shows the PL spectra obtained for gallium oxide films with different Nd contents at two different excitation wavelengths, resonantly through the Nd^{3+} levels (${}^4\text{I}_{9/2} \rightarrow {}^4\text{F}_{3/2}$) at 787 nm (thick red line) and nonresonantly at 266 nm (thin blue line). As we can see, for all samples excited by the UV light, a strong and complex green emission (GE) band centered at 500 nm is clearly observed with subbands at ~ 440 , 500, 550, and 600 nm [see Fig. 2(b)]. This band is also present for undoped but also not annealed sample [Fig. 2(a)]. However, its intensity is much lower than for the annealed one (factor ~ 40). Based on our observations, where the emission intensity for this GE band strongly increases with the annealing, the energy levels responsible for this emission could be related to Ga_2O_3 nanoclusters ($\text{Ga}_2\text{O}_3\text{-nc}$), whose formation is strongly enhanced by the annealing. These levels can be related to cluster's core but more probable to energy levels (defects or surface states) related to nanoclusters boundaries formation.

The blue side of observed emission bands in Ga_2O_3 can be explained as originating from Ga vacancies (V_{Ga}), O vacancies (V_{O}),²¹ and Ga–O vacancy pairs in Ga_2O_3 .²² In $\beta\text{-Ga}_2\text{O}_3$, the donors (V_{O}) were found to be gathered in clusters that form a donor band 40 meV below the conduction band where gallium–oxygen vacancy pair clusters form an acceptor band 420 meV above the valence band. These levels are responsible for the formation of an exciton bound as donor-acceptor pair giving rise to a blue-GE band. In addition, red band centered at about 706 nm has been already observed in $\beta\text{-Ga}_2\text{O}_3$ originating from the recombination of an electron trapped by (V_{O}) donor and a hole trapped by acceptor due to the nitrogen doping, presumably replacing oxygen in the lattice.^{23,24}

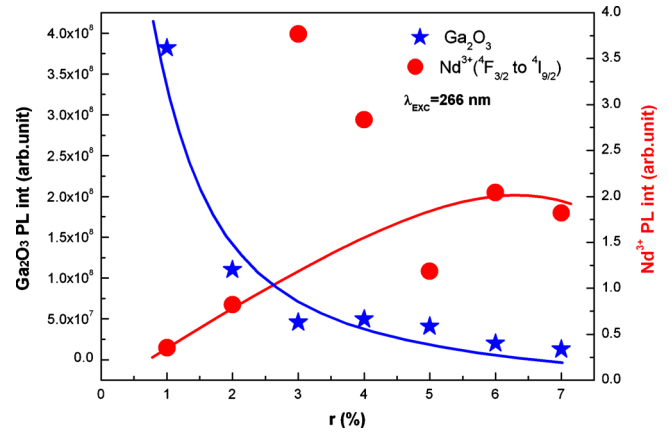


FIG. 3. (Color online) PL intensities for Nd ions and VIS emission vs surface ratio (r).

Additionally, it has been found that the emission intensity of the GE band depends on the Nd content what can be seen in more details in Fig. 3. This feature could be a consequence of more efficient coupling between the $\text{Ga}_2\text{O}_3\text{-nc}$ and Nd ions when the Nd content increases. In consequence, the averaged intensity of the $\text{Ga}_2\text{O}_3\text{-nc}$ is reduced since part of absorbed carriers is lost for Nd excitation. Unfortunately, when the Nd content increases, the shape of the emission band also changes and well resolved interference patterns are observed [see Fig. 2(c) for instance]. Despite this thickness effect, a more detailed analysis of the effect of Nd doping on the visible emission intensities has been tempted and the integrated PL intensities have been extracted and shown in Fig. 3. This figure will be discussed in the next paragraphs.

Moving to Nd related emission, at this nonresonant excitation (266 nm) emission appears only for samples with r values higher than 17.4%. Three main emission bands related to Nd ions have been observed for these samples centered at 900 nm, 1087 nm, and 1362 nm and related to transitions from ${}^4\text{F}_{3/2}$ to ${}^4\text{I}_{9/2}$, ${}^4\text{I}_{11/2}$, ${}^4\text{I}_{15/2}$ energy levels of Nd^{3+} ions, respectively, while the most intense band is at 1087 nm, which band is the most interesting from the application point of view. Above this concentration, Nd related emission strongly increases and the shape of Nd emission lines becomes narrower and characterized by a Stark effect leading to at least two sets of emission lines at characteristic energies $S_1 = 1.1462$ eV (1081 nm) and $S_2 = 1.1419$ eV (1085 nm).

On the other hand, when the samples are excited resonantly, unwanted emission band centered at 1100 nm can be observed for all Nd concentrations which band overlaps with the emission from Nd ions. We associated this band to a recombination process from the silicon substrate.²⁵ Second, as for nonresonant excitation, emission from Nd ions appears clearly when r is above 17.4% and also characterized by the evolution of the emission line shape.

When comparing both PL spectra related to the emission from the Nd ions obtained at resonant and nonresonant excitations, two phenomena are observed with the increase in Nd content. First, in both cases, the Stark splitted lines become stronger and the peaks are well separated with a spectral narrowing. This implies that with the r increase, Nd sites distribution goes from a broad one (amorphous environment)

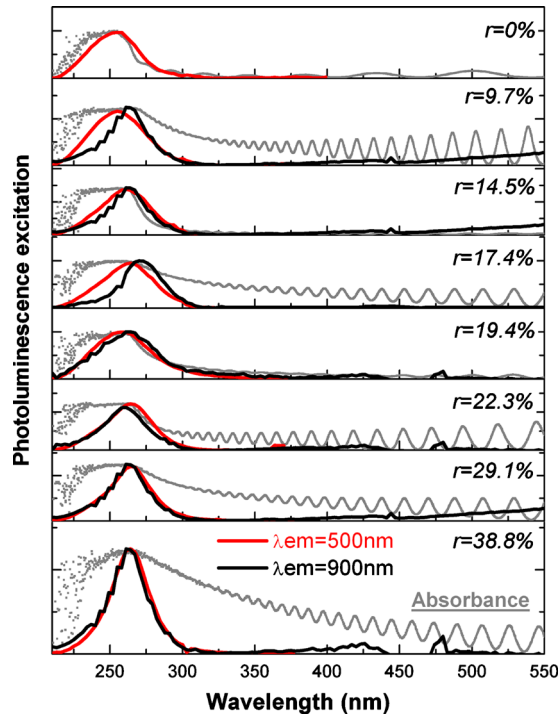


FIG. 4. (Color online) PLE spectra obtained both for emission at 500 nm (red line) and emission related to Nd ions at 900 nm (dark line) for samples containing different amount of Nd ions. Additionally, absorbance spectra have been given (dotted line).

to a sharper one (crystalline environment). Second, we deal with different contributions of the Stark splitted lines grouped at two different spectral positions, which is clearly observed for the highest r value. These results suggest that there are two main sites of Nd ions, where the ions at site- S_2 are mostly excited during a nonresonant process.

Based on these observations, we can conclude that when the gallium oxide matrix is excited resonantly (787 nm), Nd ions placed at two averaged sites (S_1 and S_2) are excited equally but when the matrix is excited nonresonantly (266 nm) most of the ions which are excited are Nd ions “coupled to element” responsible for their high energy sensitization, i.e., energy levels related to Ga_2O_3 -nc. Moreover, the improvement in emission line shapes is in agreement with our structural data which indicates that with Nd content the stoichiometry of the matrix became improved thus ions are placed in more crystalline environment.

First of all, to confirm this coupling between the sensitizing element and the Nd ions, the integrated emission intensity has been calculated for both emission bands. An evident correlation for these two emission bands (~ 500 and 900 nm) can be observed indicating that we deal with the “medium-coupling regime” since the element sensitizing the Nd ions is also responsible for the emission observed at 500 nm and only a part of excited carriers sensitizes the Nd ions.

In the second step, to define the “sensitizing element” and to confirm the excitation energy transfer from it to the Nd ions, the excitation spectra have been measured for Nd emissions at 900 and 500 nm. Figure 4 shows the excitation and the absorbance spectra obtained from the reflectance data corrected by the Si substrate reflectance. As it can be seen for

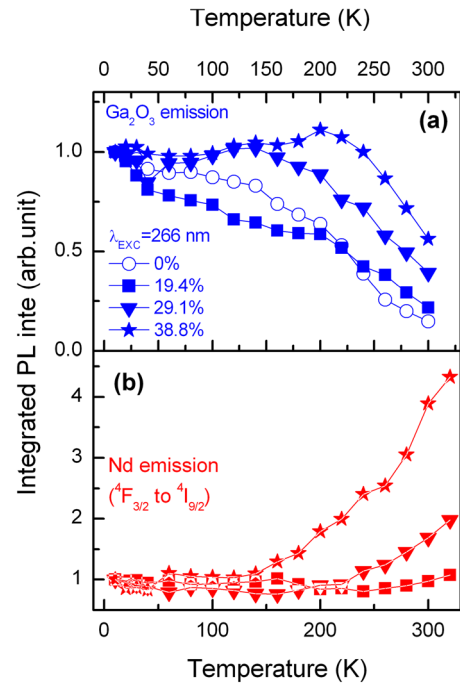


FIG. 5. (Color online) Normalized at 10K integrated PL intensities of the 500 nm (a) and 900 nm (b) bands, measured at different temperatures and obtained for samples with different Nd contents at 266 nm excitation wavelength.

each sample, the excitation spectra overlap each other and their maxima agree with the maxima of the absorbance bands centered at 250 nm (4.95 eV). These observations indicate that the excitation mechanism responsible for the emission band at 500 nm is the same as for the emission at 900 nm.

In addition, it can be seen that the excitation band position, within the experimental errors, is approximately the same for all samples. Moreover, from the absorbance spectra, evident interference patterns are clearly resolved, confirming also our previous conclusions related to the origin of multi-peaks structure of the emission band centered at 500 nm. The obtained excitation (absorption) band position is in good agreement with the values reported by other authors for the band gap of Ga_2O_3 in β phase. This indicates that the main excitation mechanism of Nd ions is through the Ga_2O_3 matrix which plays the role of a sensitizer for the Nd ions. Since we know that the Ga_2O_3 -matrix plays a crucial role in the excitation of the Nd ions, the question is to know what kind of physical process is responsible for the excitation energy transfer after the carriers are absorbed by the matrix. Is this a direct excitation energy transfer from the grains to the lanthanide ions⁴ or is this a defect mediated process?⁸ For the latter one, two main processes can be responsible for the energy transfer mediated by the defect states, namely nonradiative dipole-dipole energy transfer (Förster–Dexter) (Ref. 26) or charge (electron/hole) transfer from donor/acceptor states to Nd ions.⁹

To verify these hypotheses, the emission intensities for both emission bands at 500 and 900 nm have been recorded at different temperatures and at nonresonant excitation (266 nm). Results are shown in Fig. 5. The PL integrated intensity of the visible emission band [Fig. 5(a)] obtained for undoped

and doped with $r=19.4\%$ samples decreases with temperature and can be well fitted with a simple model describing a thermal quenching with one thermal deactivation energy equals to 43 meV and 44 meV, respectively. For doped samples with $r=29.1\%$ and 38.8% , the behavior with temperature is a bit different but the main quenching mechanism seems to be similar to the ones observed in a previous samples and can be characterized by deactivation energies equal to 54 meV and 65 meV for samples with $r=29.1$ and 38.8 , respectively.

Surprisingly, emission intensity of Nd ions has a much more different behavior when the temperature is changing [Fig. 5(b)]. In this case, the emission does not change at all until the temperature exceed approximately 150 K, which temperature corresponding to deactivation energy responsible for the quenching in emission intensities related to Ga_2O_3 grains. Based on this temperature behavior, it has been concluded that the main excitation path of Nd ions must include the charge transfer (CT) process, either the charge is directly transferred to Nd ions or via an intermediate defect states.

Taking all these results into account, excitation mechanisms of the Nd ions can be discussed in details. When the free electron will appear in the conduction band and a hole in the valence band after the 266 nm excitation (or after electrical pumping) the carriers quickly relax to the lowest levels within the energy gap of Ga_2O_3 nanocrystalline matrix (surface or defect states related to $\text{Ga}_2\text{O}_3\text{-nc}$). For all temperatures, these carriers recombine radiatively giving rise to a complex emission band centered at 500–550 nm. However, when the temperature increases (above corresponding energy of 40 meV), the recombination states become thermally depopulated to: (i) conduction band, (ii) over the potential barrier directly to Nd^{3+} ions in CT process, or (iii) over the potential barrier to the other defects energy levels which are in close spatial vicinity of $\text{Ga}_2\text{O}_3\text{-nc}$. However, based on the fact that observed Nd emission is characteristic of +3 oxidation state and direct CT from GE related donor levels to Nd requires also CT of hole to keep Nd ions optically active, we believe that the main excitation mechanism of Nd ions can be explained by two steps process via defects states. Thus, in the first step, absorbed by Ga_2O_3 matrix carriers are thermally depopulated and form an exciton localized at the energy levels related to defect states spatially close to Nd ions. In the second step, localized in this way exciton transfer its energy to Nd ion via nonradiative dipole-dipole interaction. After such a nonradiative excitation, the upper $4f$ state of Nd ions may then decay via a variety of radiative and nonradiative pathways giving rise to emission bands at 900, 1087, and 1362 nm.

Moreover, deactivation energy of 40 meV agrees very well with reported value of 40 meV below the conduction band for the oxygen vacancies related subband.¹⁰ This process decreases the number of carriers captured on nanoclusters related energy levels, what will be directly reflected in a decrease in GE band intensity and accompanied by an increase in energy transfer efficiency to Nd ions as observed in Fig. 5 and finally to increase in Nd related emission.

IV. CONCLUSIONS

Nd doped gallium oxide films of micron scale thick have been grown by magnetron sputtering. Nd concentration plays an important role in the film structure since the grain size is at least five times lower when the Nd concentration reaches 1.79%. For high Nd concentrations, Nd ions are mainly located in the surrounding of the nanoparticles of $\beta\text{-Ga}_2\text{O}_3$. The films are nonhomogeneous and contain empty cavities and small amorphous regions where the Nd content is higher than that in the grains. The optical properties have shown that a maximum intensity of Nd^{3+} emission upon optical excitation source is observed for $r=19.4\%$ corresponding to a Nd concentration slightly lower than 0.08%.

Based on the results presented above, we can conclude that there are at least two main Nd ions sites in the Ga_2O_3 film: ions being coupled to Ga_2O_3 nanoclusters, which are responsible for their sensitization and ions not coupled to any sensitizing center, which can only be excited resonantly through the Nd energy levels. Moreover, it has been shown that the main excitation mechanism of Nd ions involves a thermally activated CT process, where electrons localized in the vicinity of Ga_2O_3 nanoclusters are transferred to other states from which nonradiative dipole-dipole energy transfer to Nd ions appears. This indicates that even if Ga_2O_3 nanoclusters are the main sensitization center for Nd ions, the defect states play a crucial role in transferring excitation energy to Nd ions.

ACKNOWLEDGMENTS

The authors want to thank Jacques Perrière from the “Institut des Nanosciences de Paris” for the RBS experiments results and Łukasz Gołacki from Wrocław University of Technology for writing the software for excitation spectra analysis. This work has been supported by the Polonium project.

- ¹A. Podhorodecki, J. Andrzejewski, R. Kudrawiec, J. Misiewicz, J. Wojcik, B. J. Robinson, T. Roschuk, D. A. Thompson, and P. Mascher, *J. Appl. Phys.* **100**, 013111 (2006).
- ²G. Sęk, P. Podemski, J. Andrzejewski, J. Misiewicz, S. Hein, S. Höfling, and A. Forchel, *Appl. Phys. Express* **2**, 061102 (2009).
- ³W. Rudno-Rudziński, G. Sęk, J. Misiewicz, T. E. Lamas, and A. A. Quivy, *J. Appl. Phys.* **101**, 073518 (2007).
- ⁴A. Podhorodecki, J. Misiewicz, F. Gourbilleau, and C. Dufour, *Electrochem. Solid-State Lett.* **13**, K26 (2010).
- ⁵A. Podhorodecki, J. Misiewicz, J. Wójcik, E. Irvin, and P. Mascher, *J. Lumin.* **121**, 230 (2006).
- ⁶A. J. Kenyon, *Prog. Quantum Electron.* **26**, 225 (2002).
- ⁷A. Podhorodecki, M. Bański, J. Misiewicz, J. Serafińczuk, and N. V. Gaponenko, *J. Electrochem. Soc.* **157**, H628 (2010).
- ⁸A. Podhorodecki, G. Zatyrb, J. Misiewicz, D. Kaczmarek, J. Domaradzki, and A. Borkowska, *J. Electrochem. Soc.* **156**, H214 (2009).
- ⁹A. Podhorodecki, R. Kudrawiec, M. Nyk, J. Misiewicz, and W. Strek, *Opt. Mater.* **31**, 1252 (2009).
- ¹⁰L. Binet and D. Gourier, *J. Phys. Chem. Solids* **59**, 1241 (1998).
- ¹¹B. Liu, M. Gu, and X. Liu, *Appl. Phys. Lett.* **91**, 172102 (2007).
- ¹²R. Adair, L. L. Chase, and S. A. Payne, *Phys. Rev. B* **39**, 3337 (1989).
- ¹³T. Miyata, T. Nakatani, and T. Minami, *J. Lumin.* **87**, 1183 (2000).
- ¹⁴T. Xiao, A. H. Kitai, G. Liu, A. Nakua, and J. Barbier, *Appl. Phys. Lett.* **72**, 3356 (1998).
- ¹⁵P. Wellenius, A. Suresh, and J. F. Muth, *Appl. Phys. Lett.* **92**, 021111 (2008).
- ¹⁶E. Nogales, B. Méndez, J. Piqueras, and J. A. García, *Nanotechnology* **20**,

- 115201 (2009).
- ¹⁷S. Ohira, N. Suzuki, N. Arai, M. Tanaka, T. Sugawara, K. Nakajima, and T. Shishido, *Thin Solid Films* **516**, 5763 (2008).
- ¹⁸C. Lecerf, P. Marie, C. Frilay, J. Cardin, and X. Portier, *Mater. Res. Soc. Symp. Proc.* **1111**, 259 (2009).
- ¹⁹C. Lecerf, P. Marie, J. Cardin, A. Podhorodecki, M. banski, J. Misiewicz, and X. Portier (unpublished).
- ²⁰P. Marie, X. Portier, and J. Cardin, *Phys. Status Solidi A* **205**, 1943 (2008).
- ²¹T. Harwig and F. Kellendouk, *J. Solid State Chem.* **24**, 255 (1978).
- ²²V. I. Vasil'tasiv, Ya. M. Zakharko, and Ya. I. Prim, *Ukr. Fiz. Zh.* **33**, 1320 (1998).
- ²³Y. P. Song, H. Z. Zhang, C. Lin, Y. W. Zhu, G. H. Li, F. H. Yang, and D. P. Yu, *Phys. Rev. B* **69**, 075304 (2004).
- ²⁴H. W. Kim and S. H. Shim, *Thin Solid Films* **515**, 5158 (2007).
- ²⁵R. Ahrenkiel, S. Johnston, W. Metzger, and P. Dippo, *J. Electron. Mater.* **37**, 396 (2008).
- ²⁶D. L. Dexter, T. Förster, and R. S. Knox, *Phys. Status Solidi* **34**, K159 (1969).